

Mechanistic study on structure-property relationship of flexible organic crystals

Hongtu Zhao¹, Xiunan Zhang², Kui Chen¹, Wenbo Wu¹, Shuyu Li¹, Ting Wang^{1*}, Xin Huang¹, Na Wang¹, Lina Zhou¹, Hongxun Hao^{1,3*}

¹ National Engineering Research Center of Industrial Crystallization Technology, School of Chemical Engineering and Technology, Tianjin University, Tianjin 300072, China

² Department of Chemical and Biomolecular Engineering National University of Singapore, Singapore, 117585, Singapore

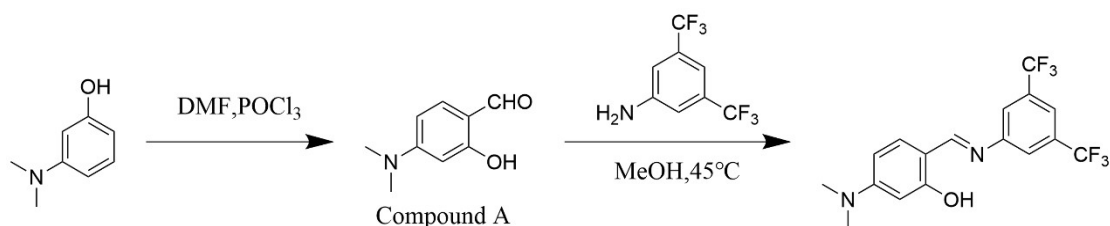
³ School of Chemical Engineering and Technology, Hainan University, Haikou 570208, China

Table of Contents

Experimental section.....	3
Molecular orbital diagrams	6
Face indexing	6
Elastic strain calculation	7
SEM images of curved MO-I crystal	8
Table of crystallographic information.....	8
Theoretical calculations	9

Experimental section

Synthesis



Scheme S1. The Synthesis of the Schiff base derivative MN

Synthesis of compound A: In a 25 mL flask, adding 3-(dimethyl amino) phenol(3.0 g, 21.8 mmol) and N,N-dimethylformamide 9mL. After stirring for 10 min in an ice-water bath, 4.2 mL of phosphorus oxychloride (45 mmol) was slowly added dropwise, and stirred at 30 °C for 30 min, then heated to 65 °C and stirred for 2 h. The above solution was poured into 42 mL of ice water, extracted three times with ethyl acetate, and back-extracted once with saturated aqueous sodium chloride solution. The organic phase was filtered through anhydrous magnesium sulfate and dried by rotary evaporation to obtain compound A as off-white powder 2.45 g (yield 72.9%). The crude product without further purification was used for subsequent synthesis.

Synthesis of compound MN: The mixture of 3,5-Bis(trifluoromethyl)aniline(0.9165 g, 4 mM),4-(dimethylamino)-2-hydroxybenzaldehyd(0.6608 g,4 mM), two drops of acetic acid and methanol(15 mL) were heated at 45 °C for 4 hours. After cooling to room temperature, the water(10 mL) were poured into flask to precipitate solid, the resulting solid was filtered. The filter cake was dried to provide 0.9995g MN as orange solid (yield 66.4%). ¹H NMR (600 MHz, Chloroform-d) δ 12.94 (s, 1H), 8.47 (s, 1H), 7.68 (td, J = 1.7, 0.9 Hz, 1H), 7.65 – 7.61 (m, 2H), 7.23 (d, J = 8.8 Hz, 1H), 6.32 (dd, J = 8.7, 2.5 Hz, 1H), 6.22 (d, J = 2.5 Hz, 1H), 3.08 (s, 6H).

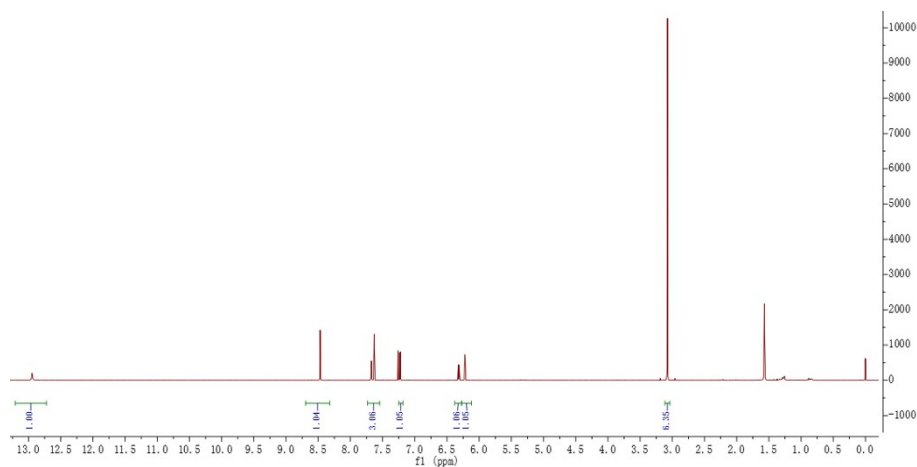


Figure S1. ¹H NMR spectrum of MN

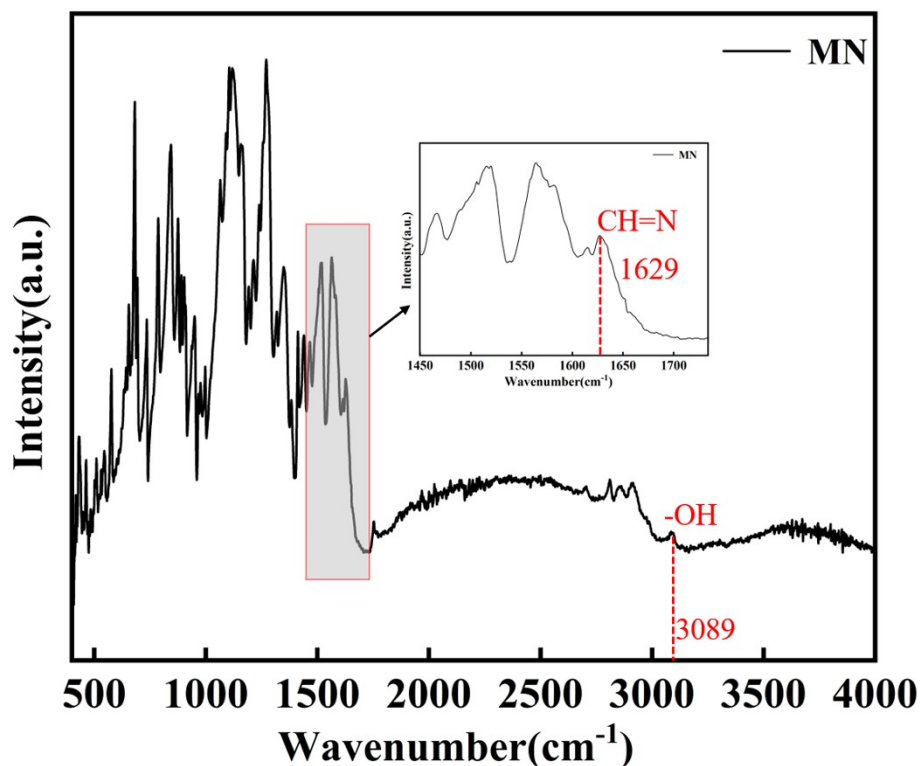
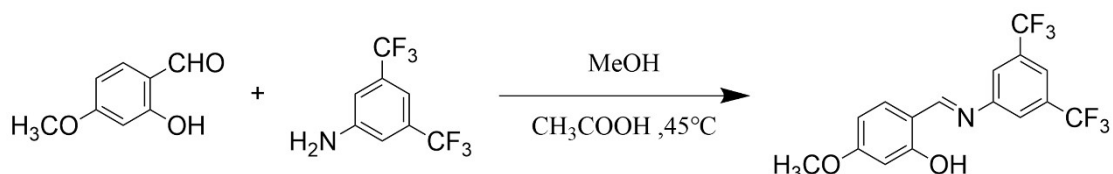


Figure S2. FTIR spectra of MN



Scheme S2. The Synthesis of the Schiff bases derivative **MO**

Synthesis of compound MO: The mixture of 2-Hydroxy-4-methoxybenzaldehyde (0.6086 g, 4 mM), 3,5-Bis(trifluoromethyl)aniline (0.9165 g, 4 mM), two drops of acetic acid and methanol (15 mL) were heated at 45 °C for 4 hours. After cooling to room temperature, the water (10 mL) were poured into flask to precipitate a yellow solid, the resulting solid was filtered. The filter cake was dried to provide 0.9719 g MO as a yellow solid (66.89%). ¹H NMR (600 MHz, Chloroform-d) δ 12.87 (s, 1H), 8.57 (s, 1H), 7.75 (s, 1H), 7.66 (d, J = 1.7 Hz, 2H), 7.33 (d, J = 8.3 Hz, 1H), 6.57 – 6.52 (m, 2H), 3.87 (s, 3H).

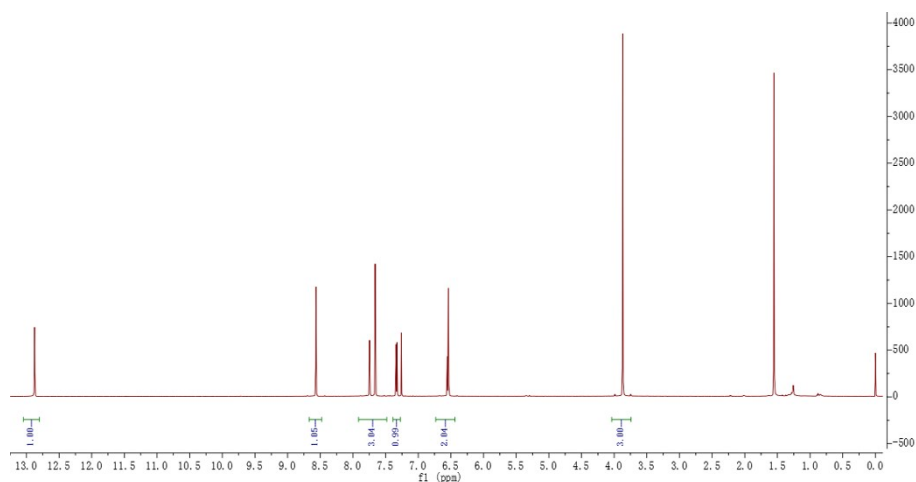


Figure S3. ¹H NMR spectrum of MO

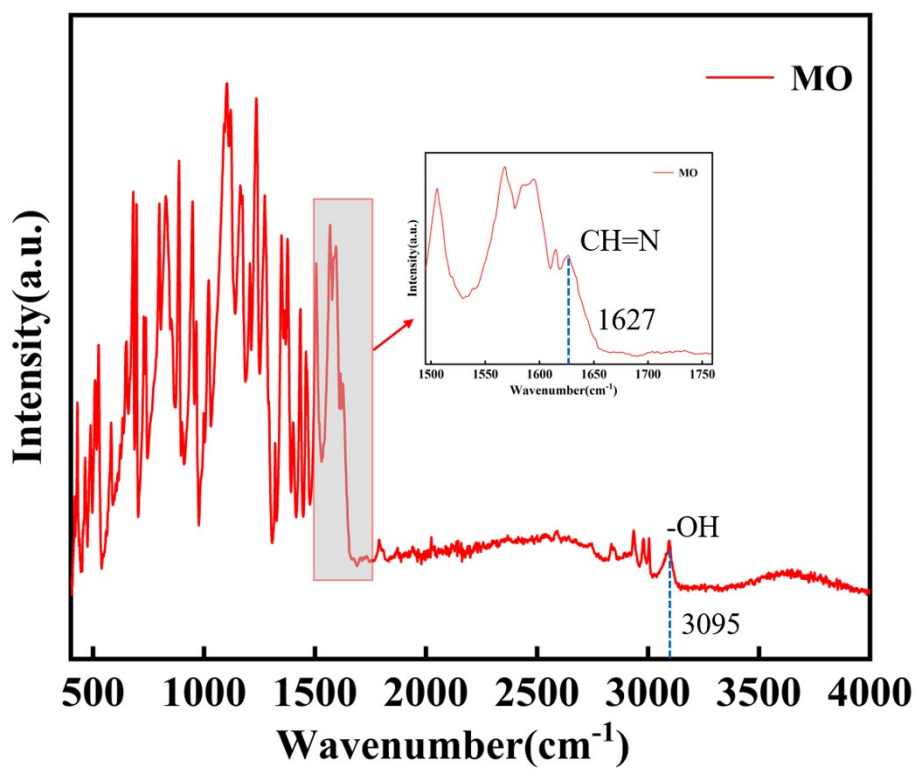


Figure S4. FTIR spectra of MO

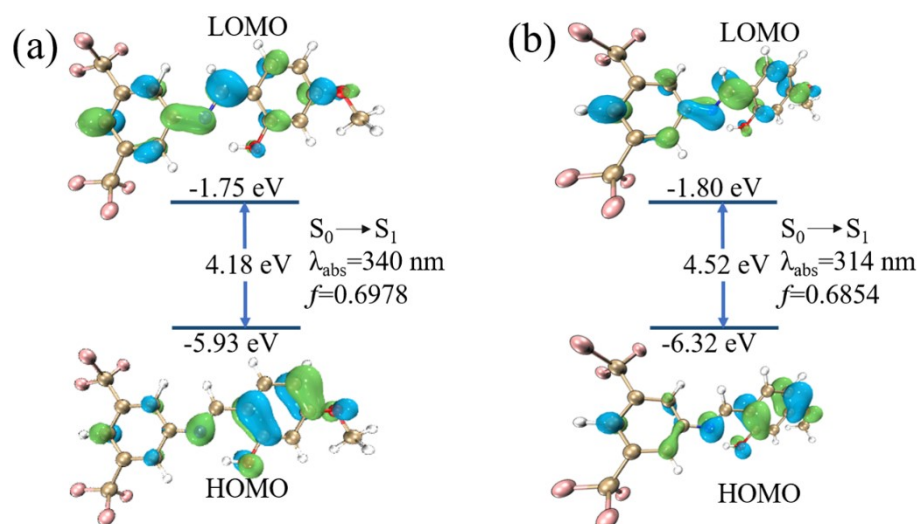


Figure S5. Molecular orbital diagrams and simulated photophysical information for (a) MO-I and (b) MO-II

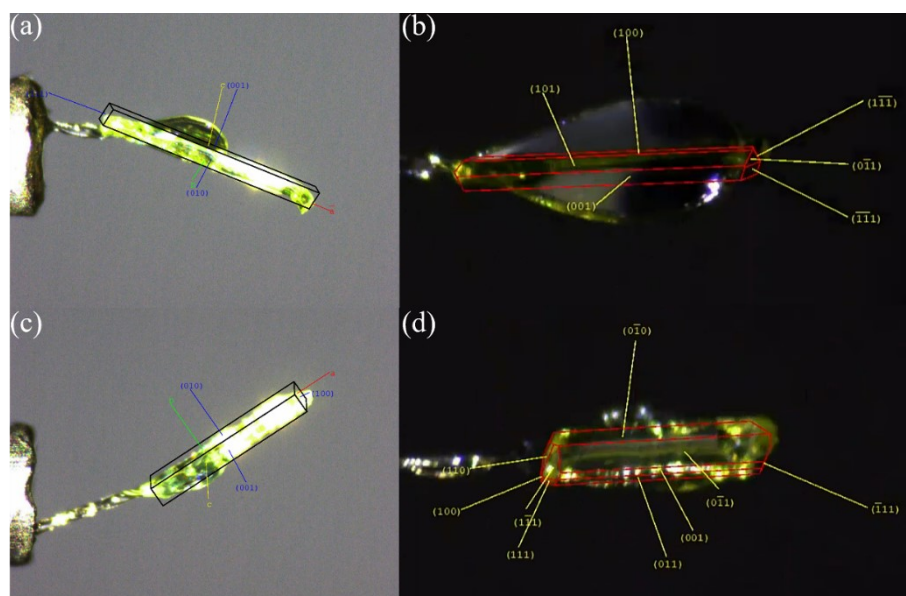


Figure S6. Face indexing image of MN-I (a), MN-II (b), MO-I (c) and MO-II (d) crystals.

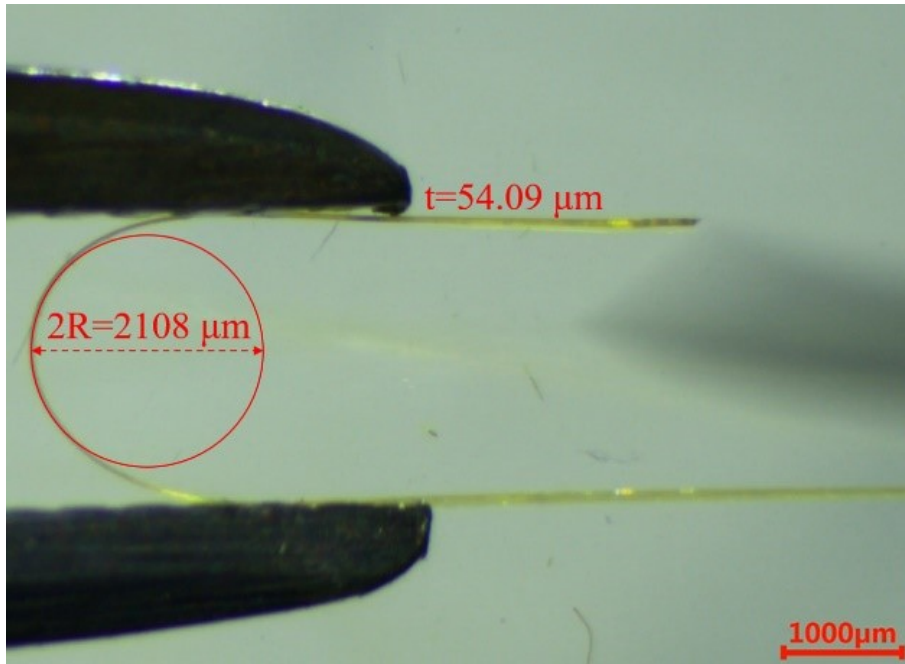


Figure S7. Elastic strain calculation of MN-I crystal along the major crystal face

$$\varepsilon = \frac{t}{2R} = \frac{54.09}{2108} \times 100\% = 2.57\%$$

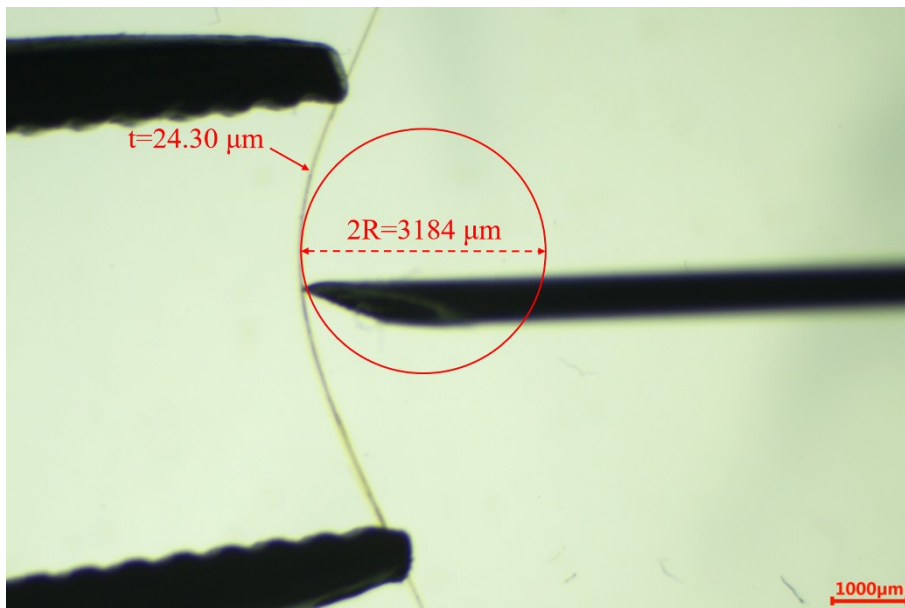


Figure S8. Elastic strain calculation of MN-II crystal along the major crystal face

$$\varepsilon = \frac{t}{2R} = \frac{24.30}{3184} \times 100\% = 0.76\%$$

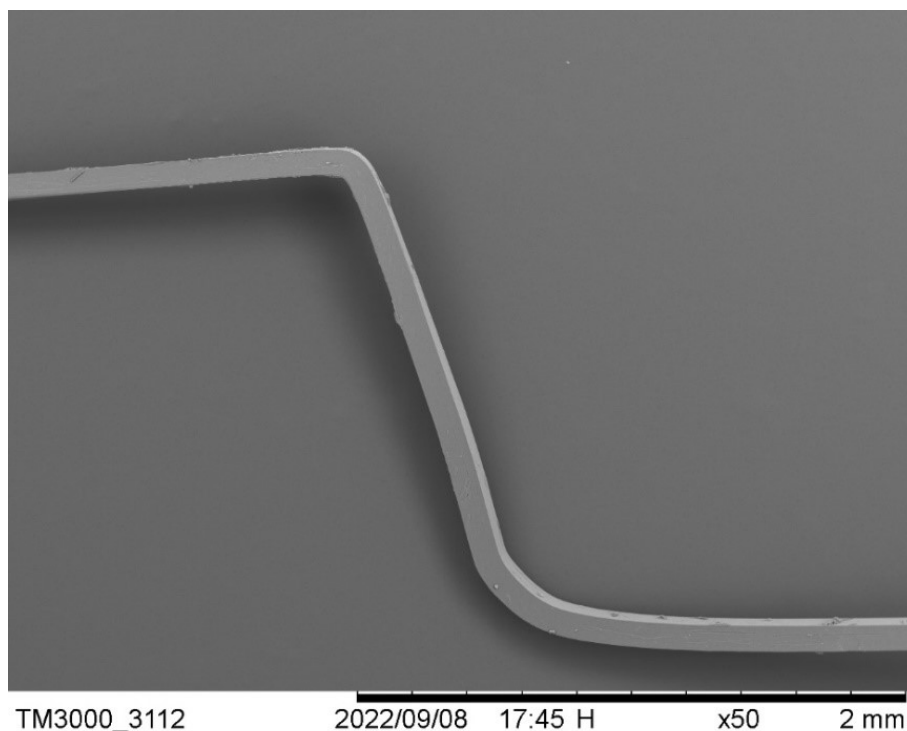


Figure S9. SEM images of MO-I crystal bent along the main crystal face, (010).

Table S1 Crystallographic Data and Refinement Details for MN and MO

Name	MN-I	MN-II	MO-I	MO-II
Empirical formula	$C_{17}H_{14}F_6N_2O$	$C_{17}H_{14}F_6N_2O$	$C_{16}H_{11}F_6NO_2$	$C_{16}H_{11}F_6NO_2$
Formula weight	376.30	376.30	363.26	363.26
Crystal system	triclinic	orthorhombic	monoclinic	monoclinic
Space group	$P-1$	$P2_12_12_1$	Cc	$P2_1/c$
$a/\text{\AA}$	4.9857(8)	6.2342(8)	4.8810(2)	7.4706(6)
$b/\text{\AA}$	10.6861(12)	14.8463(18)	36.8398(13)	30.0542(15)
$c/\text{\AA}$	16.2064(17)	18.019(2)	8.6324(3)	7.4459(7)
$\alpha/^\circ$	18.810(9)	90	90	90
$\beta/^\circ$	83.660(11)	90	104.518(4)	117.037(12)
$\gamma/^\circ$	88.872(11)	90	90	90
Volume/ \AA^3	841.84(19)	1667.8(4)	1502.67(10)	1489.1(2)
Z	2	4	4	4
μ/mm^{-1}	0.139	0.140	0.156	0.157
$\rho_{\text{calcd}}/\text{g}/\text{cm}^3$	1.485	1.499	1.606	1.620
F(000)	384	768	736	736
$\theta/^\circ$	2.530 to 25.349	2.644 to 25.350	2.211 to 31.235	2.711 to 26.370
T/K	294.15	294.15	294.15	294.15
R_1	0.0764	0.0742	0.0605	0.0542
wR_2	0.2494	0.2074	0.1772	0.1492
CCDC No.	2235342	2235345	2235337	2235341

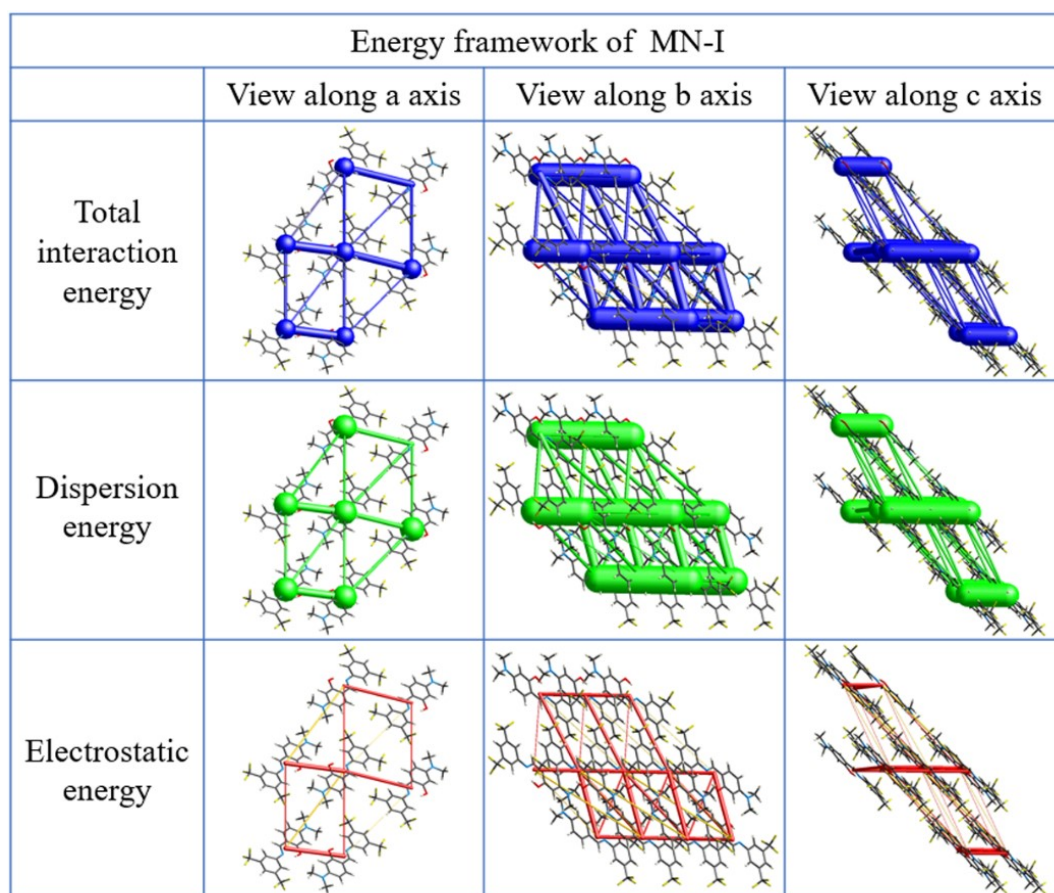


Figure S10. Three-dimensional topologies of energy framework for MN-I crystal.

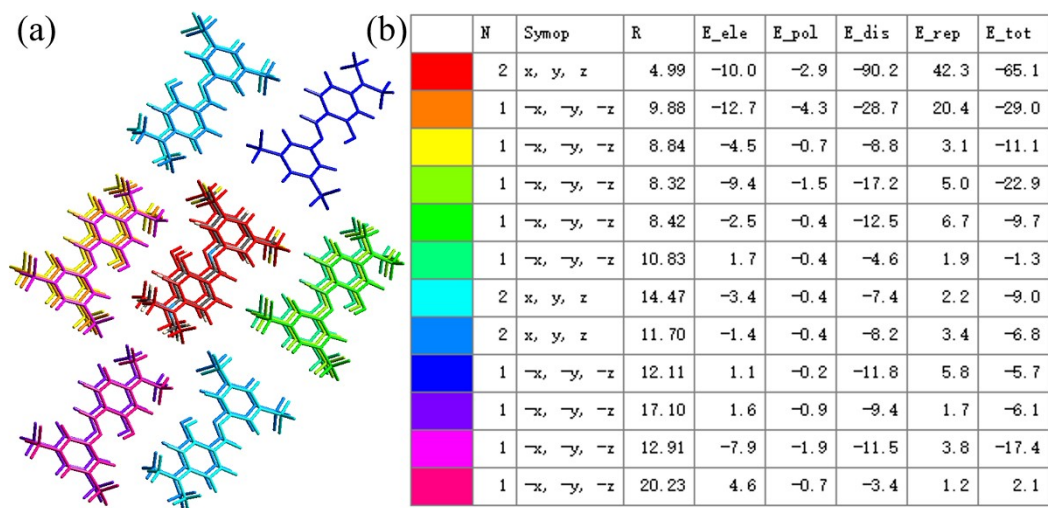


Figure S11. Molecular pairs and the interaction energies obtained from energy frameworks for MN-I crystal.

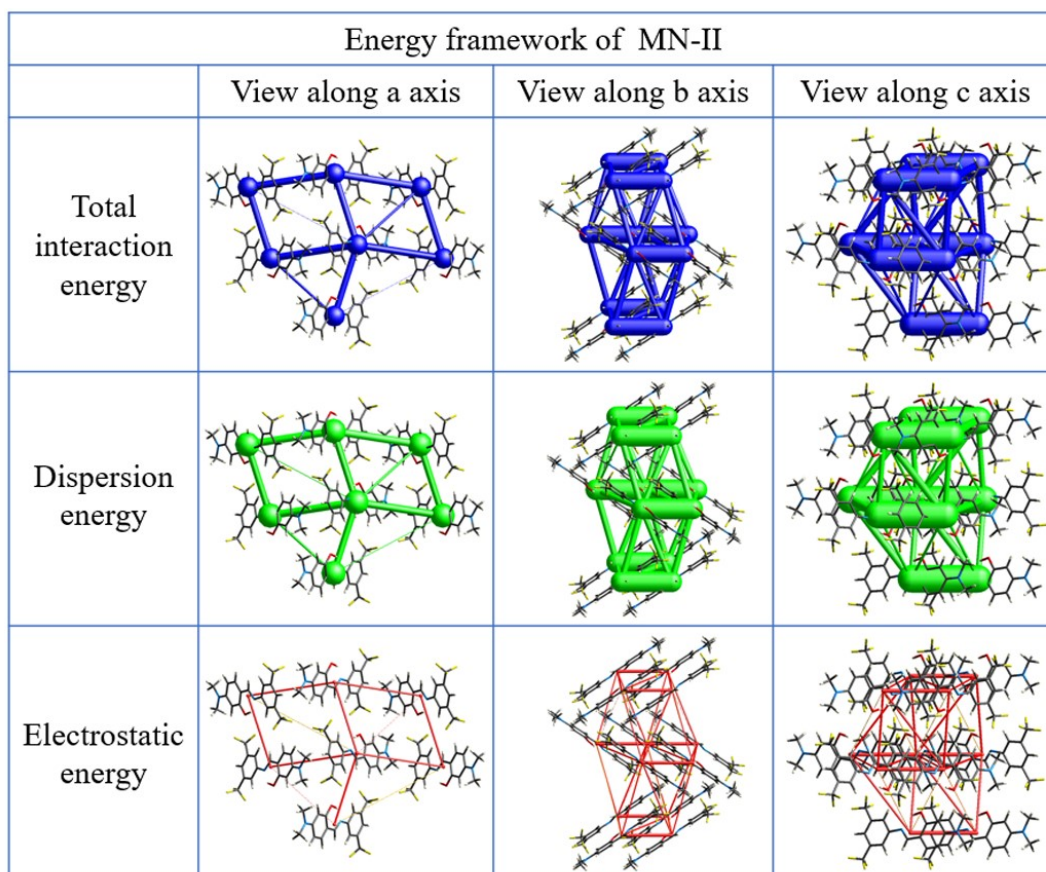


Figure S12. Three-dimensional topologies of energy framework for MN-II crystal.

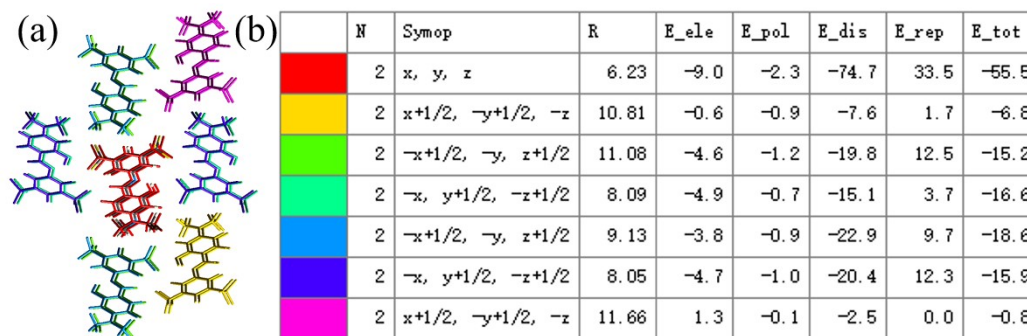


Figure S13. Molecular pairs and the interaction energies obtained from energy frameworks for MN-II crystal.

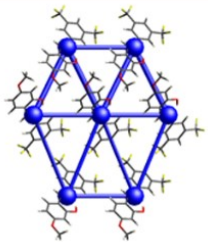
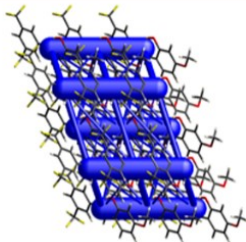
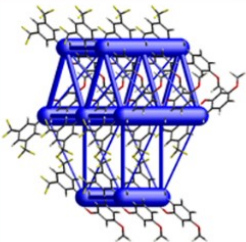
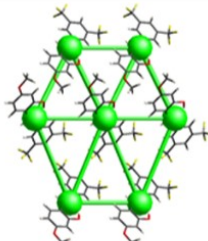
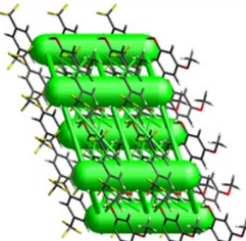
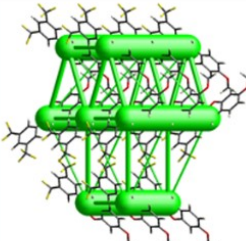
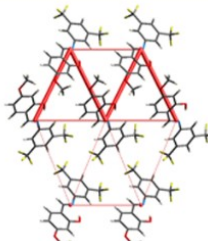
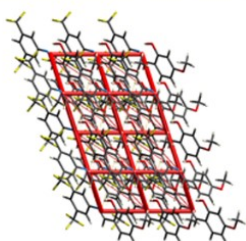
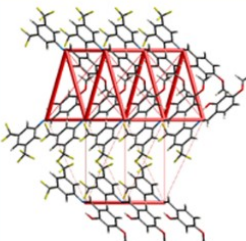
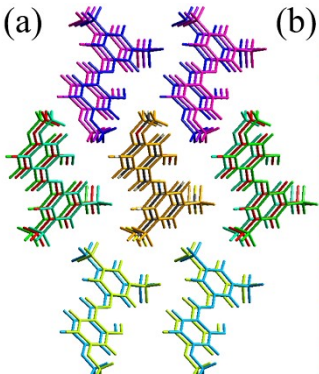
Energy framework of MO-I			
	View along a axis	View along b axis	View along c axis
Total interaction energy			
Dispersion energy			
Electrostatic energy			

Figure S14. Three-dimensional topologies of energy framework for MO-I crystal.

(a) 

(b)







	N	Symop	R	E_ele	E_pol	E_dis	E_rep	E_tot
	2	x, y, z	8.79	-3.3	-0.8	-13.2	4.5	-12.8
	2	x, y, z	4.88	-10.2	-1.8	-89.3	48.1	-60.2
	2	x, -y, z+1/2	10.23	-0.7	-0.1	-7.1	1.5	-6.1
	2	x, y, z	8.63	0.7	-0.2	-4.7	0.4	-3.2
	2	x, y, z	11.29	-2.9	-0.4	-8.8	5.6	-7.6
	2	x, -y, z+1/2	9.56	-0.9	-0.3	-15.9	4.4	-12.2
	2	x+1/2, -y+1/2, z+1/2	12.42	-1.6	-0.5	-5.8	1.9	-5.9
	2	x+1/2, -y+1/2, z+1/2	10.82	-11.9	-2.5	-17.8	19.9	-17.6
	2	x+1/2, -y+1/2, z+1/2	11.30	-0.1	-0.6	-7.7	2.4	-5.7

Figure S15. Molecular pairs and the interaction energies obtained from energy frameworks for MO-I crystal.

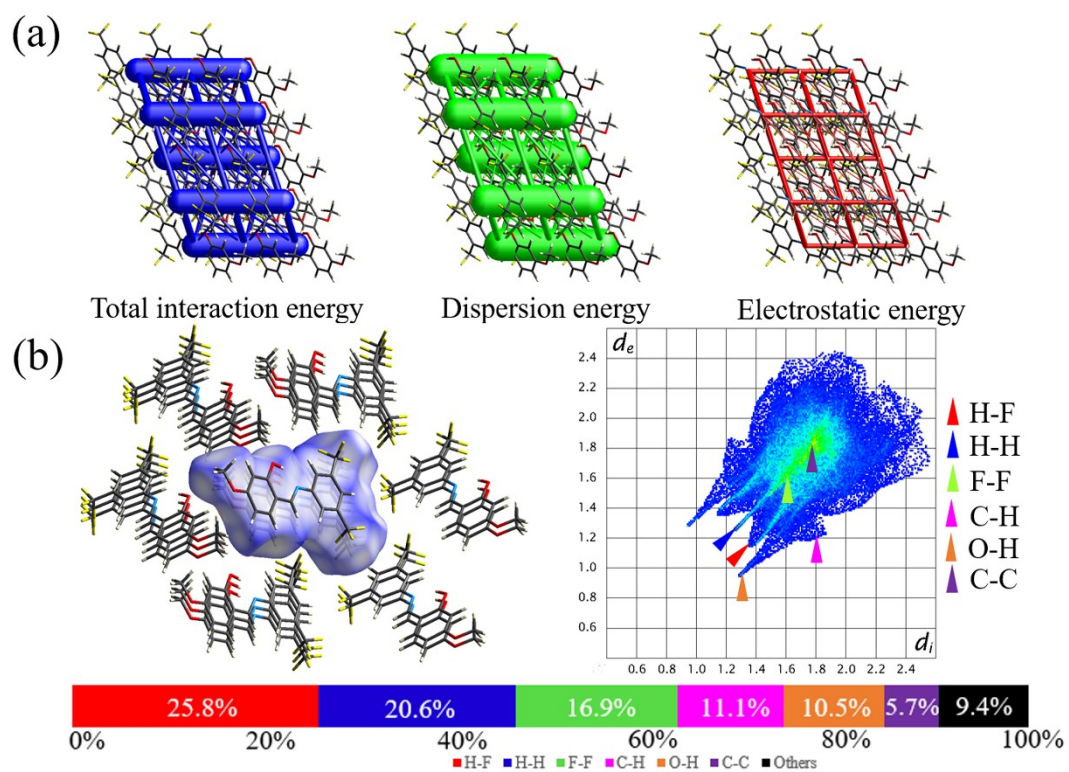


Figure S16. Energy framework (a) and Hirshfeld surface analysis (b) of MO-I crystal.

Energy framework of MO-II			
	View along a axis	View along b axis	View along c axis
Total interaction energy			
Dispersion energy			
Electrostatic energy			

Figure S17. Three-dimensional topologies of energy framework for MO-II crystal.

(a)

(b)

	N	Symp	R	E_ele	E_pol	E_dis	E_rep	E_tot
	2	x, y, z	7.79	-3.6	-1.3	-20.4	11.1	-15.7
	2	x, -y+1/2, z+1/2	11.38	0.1	-0.3	-9.1	2.4	-6.5
	1	-x, -y, -z	12.68	-0.4	-0.1	-5.7	0.9	-4.9
	2	x, y, z	7.45	0.3	-0.3	-12.8	2.6	-9.5
	1	-x, -y, -z	11.49	-0.6	-0.1	-7.7	0.8	-6.9
	2	x, -y+1/2, z+1/2	8.32	-5.7	-0.8	-35.3	17.5	-26.5
	2	x, -y+1/2, z+1/2	6.23	-14.3	-3.0	-69.3	44.4	-50.2
	1	-x, -y, -z	10.26	-0.9	-0.2	-10.4	1.7	-9.1
	2	-x, y+1/2, -z+1/2	15.24	-2.0	-0.5	-8.6	4.1	-7.4
	1	-x, -y, -z	11.69	0.4	-0.1	-8.3	1.4	-6.0

Figure S18. Molecular pairs and the interaction energies obtained from energy frameworks for MO-II crystal.